Journal of African Earth Sciences xxx (2009) xxx–xxx

Contents lists available at ScienceDirect

Journal of African Earth Sciences

journal homepage: www.elsevier.com/locate/jafrearsci

# Contrasted seismogenic and rheological behaviours from shallow and deep earthquake sequences in the North Tanzanian Divergence, East Africa

J. Albaric [a,b,*], J. Perrot [a,b], J. Déverchére [a,b], A. Deschamps [c], B. Le Gall [a,b], R.W. Ferdinand [f], C. Petit [d], C. Tiberi [e], C. Sue [a,b], M. Songo [f]

[a] Université Européenne de Bretagne, Brest, France
[b] Université de Brest, IUEM, CNRS – UMR 6538, Plouzané, France
[c] Geoazur, UNS, IRD, OCA, Nice, France
[d] Université Pierre et Marie Curie, CNRS – UMR 7072, Paris, France
[e] Université Montpellier 2, Géosciences Montpellier, CNRS – UMR 5243, Montpellier, France
[f] University of Dar Es salaam, Geology Department, Tanzania

ARTICLE INFO

*Article history:*
Received 1 April 2009
Received in revised form 1 August 2009
Accepted 4 September 2009
Available online xxxx

*Keywords:*
Earthquake sequence
Swarm
East African Rift System
Deep earthquakes
Rheology
Structural inheritance

ABSTRACT

We report preliminary results of a seismological experiment, SEISMO-TANZ' 07, which consisted in the deployment of a local network (35 stations) in the East African Rift System (EARS), North Tanzania, during 6 months in 2007. We compare two earthquake sequences (Gelai and Manyara) occurring, respectively, in the southern end of the Kenya rift and in the North Tanzanian Divergence (NTD). Only distant of ~150 km, their triggering mechanisms are different. None of the sequences depicts typical swarm or mainshock–aftershock patterns. They highlight the change in the magmatic/tectonic nature of the rift where the eastern branch of the EARS enters the Tanzanian craton. The similar shape and long-axis of the elongate sequences emphasize the preferred locus of active strain release along NE–SW discontinuities which probably root at depth into steep Proterozoic shear zones. At Gelai, the deformation is dominated by aseismic process involving slow slip on normal fault and dyke intrusion within the upper crust (Calais et al., 2008). The spatial and temporal earthquake distribution indicates a possible correlation between the Gelai crisis and the eruption of the nearby Oldoinyo Lengai volcano. At Manyara, the sequence is more uncommon, revealing a long-lasting seismic activity deeply rooted (~20–35 km depth) possibly related to stress loading transmitted laterally. The yield stress envelope modelled from the depth frequency distribution of earthquakes in the NTD is consistent with the presence of a mafic lower crust and further supports the strength increase of the rifted crust from south Kenya to the NTD.

© 2009 Published by Elsevier Ltd.

## 1. Introduction

Earthquake sequences are common features in many active rift settings. The space and time distribution of earthquakes are widely used to highlight the mechanisms that trigger them and to discuss which processes may explain their occurrences. Whereas the type of sequence is generally easily determined and often referred as swarms, aftershocks, clusters or bursts (e.g., Mogi, 1963; Sherburn, 1992; Benoit and McNutt, 1996; Vidale and Shearer, 2006; Ibs-von Seht et al., 2008; Parsons, 2008), determining their cause is not straightforward. The spatial and temporal variability of seismic deformation and its relationship with aseismic processes such as magma injections, slow slip, static or dynamic stress triggering are generally poorly understood owing to the lack of accuracy on spatial and temporal evolution of deformation and on the rheological setting. An open question is also whether and how long earthquake clustering is expected to persist, with important consequences on seismic hazard forecasting.

Continental rifts are known to provide evidence since long for various types of earthquake sequences, either as mainshock–aftershock sequences or as swarms. From earthquake series captured in various modern rift systems (Rio Grande, Kenya and Eger), Ibs-von Seht et al. (2008) have recently suggested that swarm activity is mostly restricted to rift valleys at shallow depth and are influenced by large-scale fracture or shear zones intersecting the rifts, which are assumed to favour intrusions of upper mantle into the crust. A similar pattern is reported in the Baikal rift, but some "swarm-like" sequences identified there depict even much longer time series (several years) and develop off the main rift axis and at depth as large as 23 km (Déverchère et al., 1993; Solonenko et al., 1997).

In 2007, a French–Tanzanian seismic experiment (SEISMO-TANZ' 07) took place from June 1st to November 20, in the North

* Corresponding author. Address: Université Européenne de Bretagne, Brest, France.
*E-mail address:* albaric@univ-brest.fr (J. Albaric).

1464-343X/$ - see front matter © 2009 Published by Elsevier Ltd.
doi:10.1016/j.jafrearsci.2009.09.005

Please cite this article in press as: Albaric, J., et al. Contrasted seismogenic and rheological behaviours from shallow and deep earthquake sequences in the North Tanzanian Divergence, East Africa. J. Afr. Earth Sci. (2009), doi:10.1016/j.jafrearsci.2009.09.005

UNCORRECTED PROOF

Tanzanian rift, at the southern end of the eastern branch of the East African Rift System (EARS) (Fig. 1A). This branch depicts a general, large scale southerly-propagating rift pattern (Le Gall et al., 2008, and references therein). At about 2.5°S, the main axial valley splits into several zones of deformation of different strikes, forming the so-called North Tanzanian Divergence (NTD) (Dawson, 1992). Fortuitously, the SEISMO-TANZ' 07 temporal seismic network has captured simultaneously two earthquake sequences, called hereafter Gelai and Manyara, located, respectively, in the volcanic area of the NatronValley and at the contact of the Tanzanian Archaean craton near Lake Manyara (Fig. 1A). The aim of this study is to take advantage of this exceptional opportunity to contrast deformation mechanisms and rheological settings during synchronous, yet spatially discrete magma-rich and magma-poor continental rifting episodes. We intend to describe the main spatial and temporal patterns of these two sequences, to underline their specificities, similarities and differences, and to compare them to other sequences captured in continental rifts in order to infer rheological implications and possible triggering mechanisms.

## 2. Geological and seismological settings

### 2.1. Tectono-magmatic framework

The Gelai and Manyara sequences take place at the southern end of the southerly-propagating eastern branch of the EARS (Fig. 1A) where faulting and magmatism initiated at around 15 Ma (Baker and Mitchell, 1976). They occur in two contrasted rift settings, resulting from the splay of the axial rift valley southwards into the 400 km-wide NTD (Dawson, 1992):

(1) To the north, the Gelai earthquakes lie within the Natron axial trough which forms a 50- to 60-km wide westerly-facing half-graben, slightly offset to the SW with respect to the Magadi linear N–S rift valley in south Kenya (Fig. 1A). There, strain history over the last 15 Myr is marked by repeated episodes of extensional faulting and magmatism (Cerling and Powers, 1977; Crossley and Knight, 1981), producing a limited extension (<15–20%) and little crustal thinning, esti-

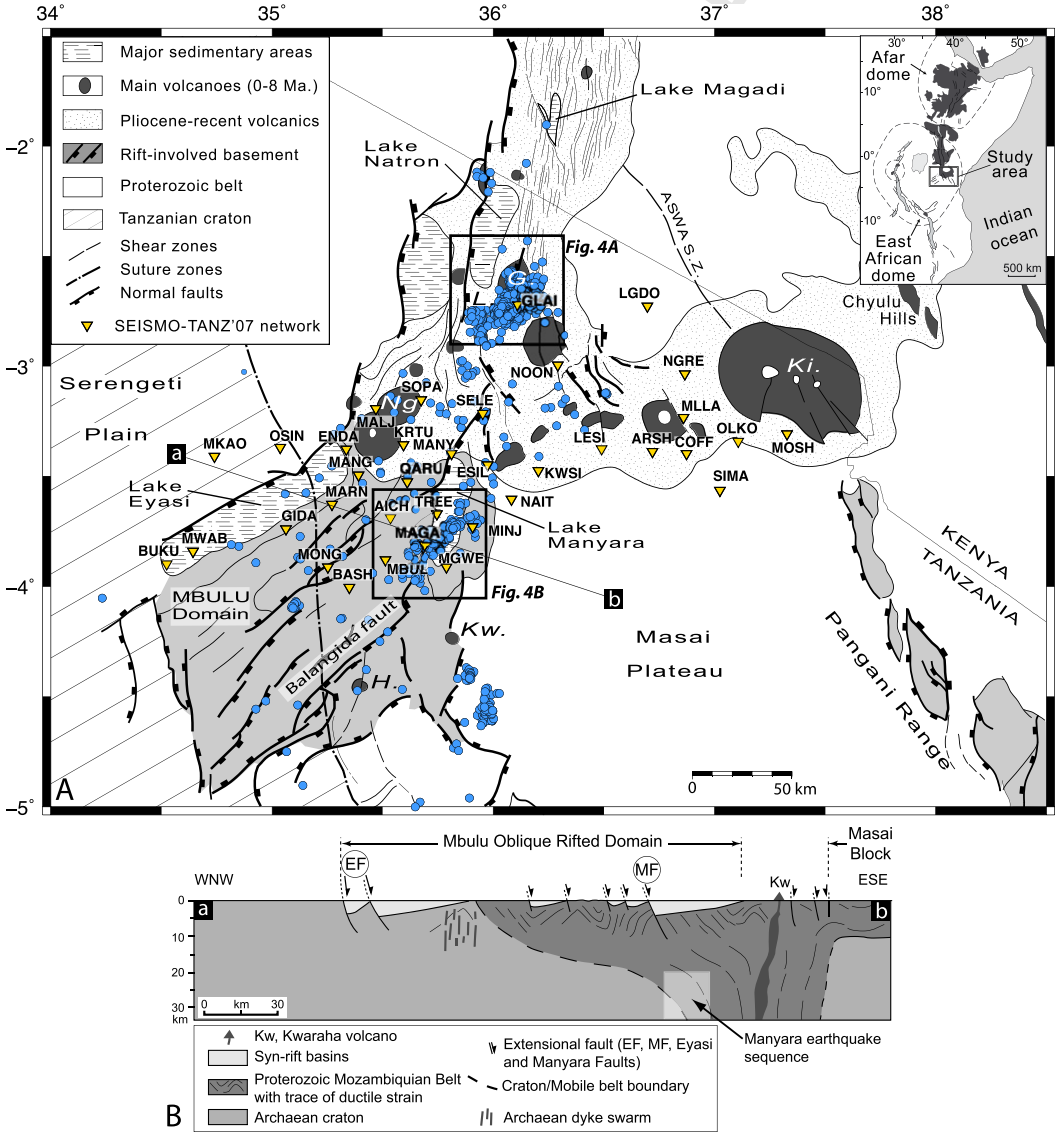



**Fig. 1.** (A) Structural sketch map of the NTD (modified from Le Gall et al., 2008) with SEISMO-TANZ' 07 network and seismicity (blue circles) recorded from June to November 2007. NOON and GLAI were only installed in August. (B) 2D-cross-section (a–b on A) of the western arm of the NTD showing the root of the frontal Mozambiquian Belt along a suture zone deepening between two cratonic blocks. The approximate location of the root zone does not permit to definitely assess whether the Manyara sequence occurs within the craton or in the Mozambiquian Belt. The Kwaraha volcano and its inferred magma conduits are projected from their southern location. ASWA SZ, ASWA shear zone; G., Gelai; H., Hanang; Ki., Kilimanjaro; Kw., Kwaraha; L., Oldoinyo Lengai; Ng., Ngorongoro; EF, Eyasi fault; MF, Manyara fault.

Please cite this article in press as: Albaric, J., et al. Contrasted seismogenic and rheological behaviours from shallow and deep earthquake sequences in the North Tanzanian Divergence, East Africa. J. Afr. Earth Sci. (2009), doi:10.1016/j.jafrearsci.2009.09.005

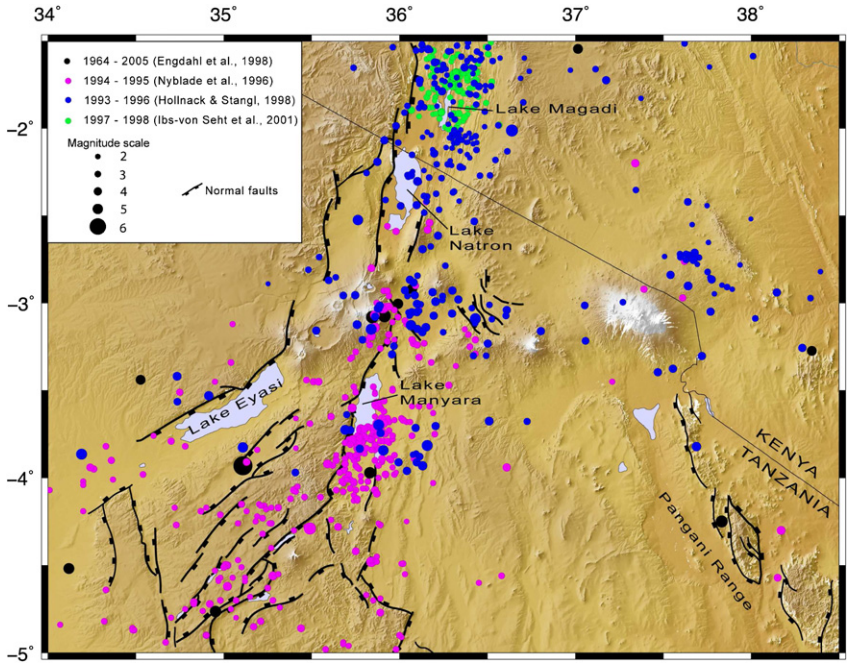



**Fig. 2.** Map of the North Tanzanian Divergence showing topography, major faults and seismicity from different catalogues (circles with a colour code) available before June 2007, beginning of the SEISMO-TANZ' 07 experiment. The diameter of the circles is proportional to the magnitude of the events.

UNCORRECTED

mated at ca. 5 km beneath the axial valley (Prodehl et al., 1994; Last et al., 1997). During the last 1 Ma, a dense extensional fault grid cuts through the 1.6–0.8 Ma-old Magadi trachybasalts on the shallow flexural side of the half-graben to the east (Crossley, 1979). The Gelai seismic sequence occurs on the southern edge of the 1.0 Ma-old Gelai volcano (Evans et al., 1971), i.e. immediately south of the axial grid fault pattern, in a subdued area where the basaltic rift floor is buried by recent deposits.

(2) To the south, the Manyara earthquakes outline the southern shoreline of Lake Manyara (Fig. 1A). The majority of the events are 5 km east of the Manyara east-facing master fault which bounds to the east the so-called Mbulu oblique rifted domain. The latter and the Pangani rift branch on the eastern side of the Masai plateau form the western and eastern arms of the NTD, respectively (Le Gall et al., 2008).

The NTD marks a sharp transition between the magmatic and amagmatic rifts, characterized by the Neogene E–W transverse volcanic chain extending over more than 200 km from the Ngorongoro to the Kilimanjaro volcanoes (Nonnotte et al., 2008, Fig. 1A). In contrast with the Magadi–Natron magmatic rift and the Kilimanjaro-Ngorongoro transverse volcanic belt, the NTD is devoid of synrift volcanism, except the discrete Hanang (1.5–0.9 Ma) and Kwaraha (1.5–0.7 Ma) volcanoes on the eastern edge of the Mbulu faulted domain (Bagdasaryan et al., 1973, Fig. 1). The Mbulu rift arm continues the Magadi–Natron axial trough approximately 150 km to the S–W, but with striking changes in structural style. These variations typify a nearly 100 km-wide oblique zone of diffuse strain, dominated by the SE- and E-facing Eyasi and Manyara bounding faults, respectively. The diamond-shaped extensional fault block pattern in the Mbulu rift arm crosscuts the boundary between the Archaean craton and younger Proterozoic mobile belts (Fig. 1), cutting at high angle through strong NE–SW-trending magmatic dykes and ductile Archaean fabrics (Barth, 1990). According to aeromagnetic modelling, further supported by previous field observations in Kenya (Shackleton, 1993), the eastern edge of the Tanzanian craton should extend at depth, ca. 50 km further east of the exposed contact, beneath a shallow wedge of westerly-directed metamorphic thrust-nappes (Ebinger et al., 1997). The overall structure of the Proterozoic thin-skinned pile is tentatively depicted on a 2D-cross-section as a thrust-nappe system steepening and rooting at depth, below Lake Manyara, along a narrow suture zone squeezed between the buried edge of the Tanzanian craton and the N–S margin of the Masai plateau (Fig. 1B). The Archaean origin of the latter is deduced from its amagmatic and aseismic nature, in addition to its unrifted topography and NE–SW Archaean-type magnetic fabrics (Ebinger et al., 1997).

### 2.2. Seismological setting

The NTD was for the first time seismically monitored at local scale with the SEISMO-TANZ experiment. A general view on the overall seismic activity is provided by global catalogues, as the updated EHB catalogue which shows the location of earthquakes since 1965 spreading over the Kenya rift and the NTD (Engdahl et al., 1998, $M \geqslant 4.3$, black dots, Fig. 2). In southern Kenya, a permanent seismic array deployed since 1990 has recorded 2000 events between October 1993 and August 1996 with local magnitudes reaching 5 (Hollnack and Stangl, 1998, blue dots, Fig. 2). A dense seismic survey of the Lake Magadi area, north of Lake Natron, allowed to locate more than 300 events between November 1997 and June 1998 (Ibs-von Seht et al., 2001, green dots, Fig. 2[1]). Finally, Nyblade et al. (1996) have installed a regional-scale network of 20 stations from June 1994 to May 1995 across the Proterozoic Belts and the Tanzanian craton, allowing to locate about 2000 events in North Tanzania (pink dots, Fig. 2). The completeness level of these data is of magnitude ($M_L$) 2–2.5 (Langston et al., 1998).

From these catalogues available before June 2007, it is worth to note the clear tendency of earthquakes to cluster around Lake Mag-

[1] For interpretation of color in Fig. 2, the reader is referred to the web version of this article.

Please cite this article in press as: Albaric, J., et al. Contrasted seismogenic and rheological behaviours from shallow and deep earthquake sequences in the North Tanzanian Divergence, East Africa. J. Afr. Earth Sci. (2009), doi:10.1016/j.jafrearsci.2009.09.005

adi and southern Lake Manyara, whereas seismicity remains apparently rather sparse, low magnitude or spread over the other parts of the NTD and the southern Kenya rift (Fig. 2). Especially, no seismic activity was identified in the vicinity of the Gelai and Lengai volcanoes in this period of time. However, one has to be aware of the large heterogeneities of these catalogues, either in magnitude range or in space and time coverage. Furthermore, remaining uncertainties on hypocenters from regional catalogues (Nyblade et al., 1996; Hollnack and Stangl, 1998) also limit the availability of connections with known faults at the surface and of shape aspects of earthquakes sequences.

## 3. The SEISMO-TANZ' 07 experiment

### 3.1. The seismic network

The SEISMO-TANZ' 07 experiment is a French–Tanzanian collaboration, launched in 2007, consisting in the deployment of a local seismological network in North Tanzania for 6 months. The equipment came from the french national pool Lithoscope and french laboratories (Geoazur, Nice; Domaines Océaniques, Brest).

It was launched in February 2007 with a site recognition and followed in June by the installation of 35 stations (Fig. 1A). In August, we did a maintenance and retrieval data mission during which the station KWSI was moved to GLAI and a new one, NOON, was installed. Indeed, the KWSI site was damaged, so no more safe, and we wanted to extend the network to the Natron region, affected by a $M_w$ 5.9 earthquake in July, without changing completely its configuration. At the end of November, most of the stations were removed and some of them moved to the North from which data are not studied here.

The equipment is composed of continuous digital recording systems with GPS time control (TITAN, mini-TITAN and OSIRIS). The sample rate was 125 Hz everywhere but at station MOSH where it was 62.5 Hz. This site is located at the extreme eastern side of the region where only teleseismic observations were expected. Different sensors were used: 2 short period (L4C – 1 Hz and L22 – 2 Hz), 20 enlarged bands (Noemax (20 s–50 Hz) and Lennartz Le3D (5 s–50 Hz)) and 13 broadband (Güralp CMG 40T (60 s–50 Hz) and Güralp CMG 3T (120 s–50 Hz)). The power was generally supplied by solar panels charging batteries. Five stations (ARSH, BUKU, LESI, OLKO, SELE) were out of order during nearly all the period, and a lot of data were not recovered from others because of different problems (robbery, weather, animals, hard disk). However, it is more than 200 Gb of data we recovered and processed for this temporary experiment.

The network configuration was designed to study the seismotectonics of the two most seismic active ending branches of the NTD and to characterize the crustal structure at a larger scale, beyond the E–W volcanic belt to the south (Figs. 1 and 2). The majority of the stations were then deployed around the Eyasi and Manyara escarpments with a mean spacing of 20 km and generally greater (30–40 km) around the Meru and Kilimanjaro volcanoes (Fig. 1A).

### 3.2. Data processing

We first ran a STA/LTA (short term average/long-term average) trigger algorithm on the continuous recording raw data corrected from the time drift of the internal clock. Events were converted to the SEISAN software format, used to pick *P*- and *S*-wave arrivals and evaluate the signal duration (Havskov and Ottemöller, 2008). Duration magnitude was calculated with the Lee et al. (1972) coefficients, valid for $M_c \leqslant 3.5$. The largest magnitudes reported come from the NEIC catalogue.

The preliminary earthquake location and magnitude determination were performed with the location program HYPOCENTER (Lienert and Havskov, 1995). We used a simple velocity model derived from previous studies in the area, including seismic refractions in south Kenya (KRISP, 1991; Birt et al., 1997; Prodehl et al., 1997), receiver function analysis (Last et al., 1997; Julia et al., 2005) and $P_n$ travel time inversion (Brazier et al., 2000; Nyblade and Brazier, 2002). It consists of three crustal layers with $V_p = 5.9$ km s$^{-1}$ from 0 to 14 km depth, $V_p = 6.5$ km s$^{-1}$ from 14 to 27 km and $V_p = 6.8$ km s$^{-1}$ from 27 to 37 km depth. The upper mantle velocity is 8.3 km s$^{-1}$.

We deduced a mean $V_p/V_s$ of 1.72 from both the Wadati diagram and the Chatelain method (Chatelain, 1978).

More than 2000 earthquakes were located during the 6 months of the experiment, using records from by a minimum of 6 stations (Fig. 1A). About 80% are due to the Gelai crisis, described in the next section. Unfortunately, the majority of these events are outside the network and had a"hiding effect" on the micro-seismicity of the Manyara–Eyasi tectonic system, particularly in July and for the two first weeks of August. The mean absolute errors of the 2068 events plotted in Fig. 1A are ±3.0 km in latitude, ±1.9 km in longitude and ±2.9 km in depth (Fig. 3).

### 3.3. Hypocenter relocation

We have applied the double-difference algorithm (DD) of Waldhauser et al. (2000) to obtain precise relative locations for the Manyara sequence. The DD technique is based on the assumption that the difference of travel times between two sufficiently close earthquakes, recorded at a common station, is free of the unmodelled velocity structure effects. Travel-time differences for pairs of earthquakes are therefore directly inverted for event separation, allowing to determine accurate relative hypocenter locations.

As for the absolute location, the performance and the reliability of the relative location is limited by the data quality (Waldhauser et al., 2000). To be stable, it requires a sufficient number of differential arrival times and a favourable network configuration. For the Gelai sequence, its mean azimuthal coverage and nearest station distance are 234° and 58 km, respectively. Hence, this system is not stable enough and requires too large damping to get relevant results from DD relocation.

The case of Manyara sequence is more suitable for the DD relocation, with its mean azimuthal coverage and nearest station dis-

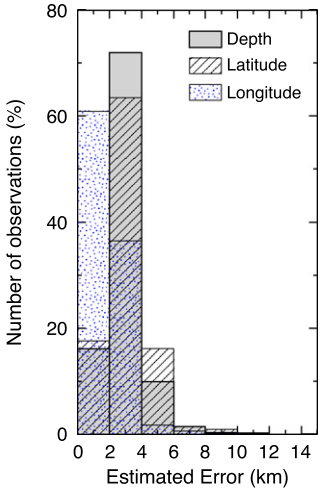



**Fig. 3.** Distribution of epicentral and depth absolute errors for the 2068 events plotted in Fig. 1A. The errors are greater in latitude than longitude because of the location of most of the earthquakes north of the network.

UNCORRECTED PROOF

Please cite this article in press as: Albaric, J., et al. Contrasted seismogenic and rheological behaviours from shallow and deep earthquake sequences in the North Tanzanian Divergence, East Africa. J. Afr. Earth Sci. (2009), doi:10.1016/j.jafrearsci.2009.09.005

tance equal to 153° and 12 km, respectively. We used *hypoDD* with the singular value decomposition method and a re-weighting approach to relocate these events from the *P* and *S* arrival-time readings (Waldhauser et al., 2000; Waldhauser, 2001). To build up a network of well connected events, we have only considered pairs with corresponding phases observed at least at 8 common stations.

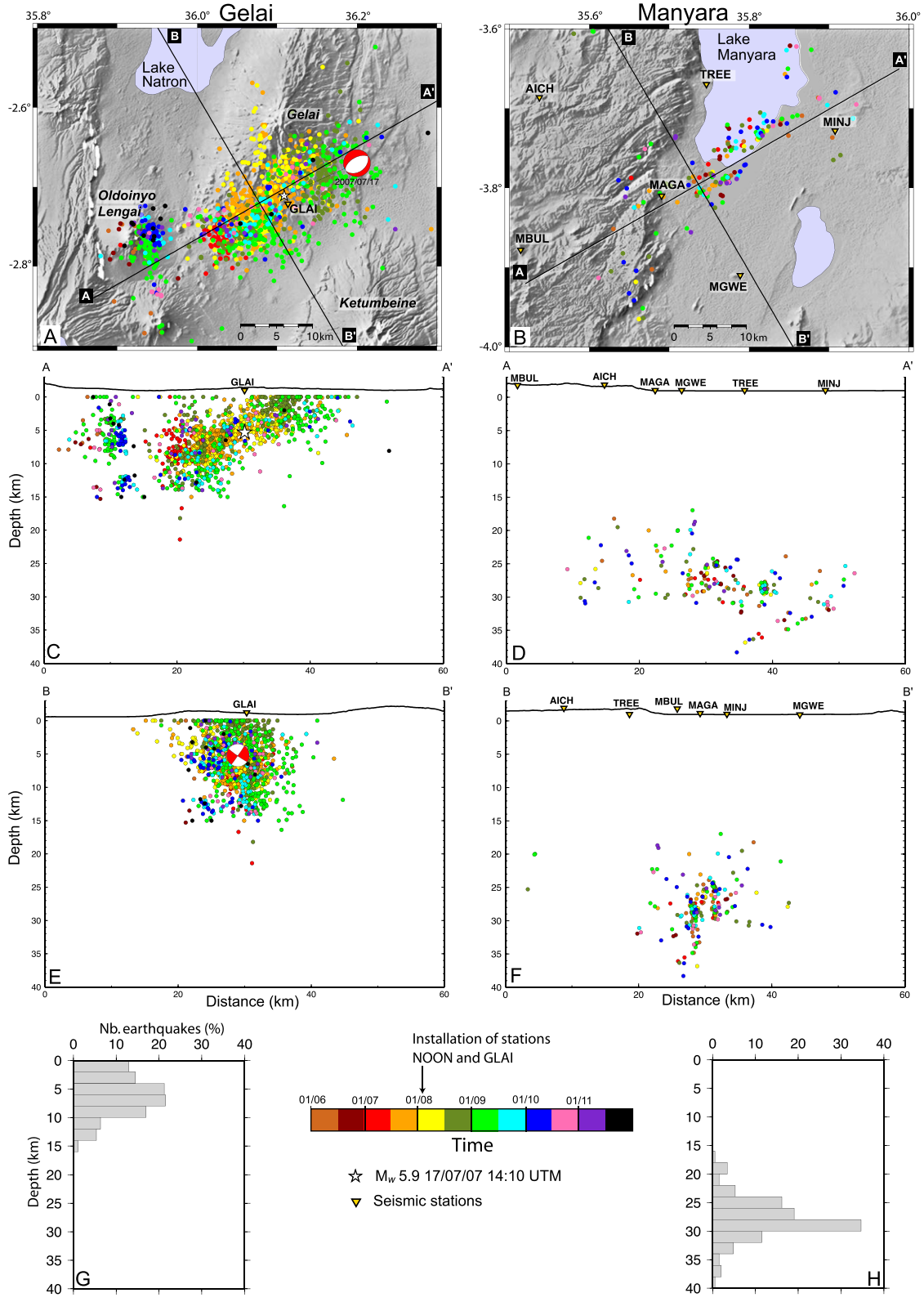



**Fig. 4.** Distribution of the Gelai (left) and Manyara (right) seismic sequences on maps (A and B) and 2D-cross-sections oriented parallel (C and D) and orthogonal (E and F) to the NE–SW axis of the active zones. G and H are the depth distribution of earthquakes each 2 km. On map (B) line A–A′ roughly separates two alignments of epicenters striking in the same direction (see text for details). The seismicity in the Gelai region comes from the absolute location of 1418 events. The Manyara sequence was relocated with the double-difference algorithm (Waldhauser et al., 2000) and comprises 211 events. The focal mechanism of the main event on map (A) and cross-section E ($M_w$ 5.9, Strike 241°, Dip 55°, Rake -85°).

Please cite this article in press as: Albaric, J., et al. Contrasted seismogenic and rheological behaviours from shallow and deep earthquake sequences in the North Tanzanian Divergence, East Africa. J. Afr. Earth Sci. (2009), doi:10.1016/j.jafrearsci.2009.09.005

The procedure has provided a relocated data set of 211 events with a mean relative error of 145 m in longitude, 177 m in latitude and 269 m in depth (Fig. 4B).

## 4. Two earthquake sequences captured by the SEISMO-TANZ' 07 network

The local seismicity recorded in the NTD in 2007 is heterogeneously distributed. Three small areas, aligned in the direction of the Kenya Rift (N–S) undergo a high level of seismicity compared to some wide faulted and volcanic regions (Eyasi and Pangani arms, E–W volcanic transverse belt, Fig. 1A). The aim of this section is to characterize and compare the two earthquake sequences captured in the Natron–Gelai and Manyara areas (rectangles in Fig. 1A) by our seismological network in order to highlight different deformation processes occurring at distance less than 150 km. Indeed, their characteristics, in terms of spatial and time distribution, frequency characteristics of the waveforms and depth distribution of earthquakes, present differences that could be related to their origin: aseismic (slow slip and dyke intrusion) in the case of the Gelai sequence (Calais et al., 2008; Baer et al., 2008) and probably purely tectonic in the case of Manyara.

### 4.1. The Gelai sequence

#### 4.1.1. Spatial and time distribution

This sequence represents more than 1200 earthquakes located at the limit between the Kenya rift and the NTD, on the southern side of the Gelai volcano (Figs. 1A and 4A). Before July 12, no seismicity was detected in this region by our network, except under the Oldoinyo Lengai volcano (Figs. 4–6). The seismicity rate is maximum on July 17, when the major event of the sequence occurred ($M_w$ 5.9; 14:10, UTC) but remains important in August and September (Fig. 5). Less than two events per day were recorded when most of the stations were removed in November. However, two earthquakes of $M_w$ 5.3 and $M_w$ 4.7 occurred in December, showing that the crisis was still going on. The decrease of the seismic rate is not clearly comparable to a mainshock–aftershock sequence as described by Mogi (1963), with peaks of seismicity before and after the largest shock (Fig. 5). It is neither a classically defined swarm because of the occurrence of a large event (Mogi, 1963; Benoit and McNutt, 1996).

The earthquakes depict an elongated shape in the N–E direction that rotates clockwise from ~N30°E in July to ~N60°E from mid-August (Fig. 4A). Under Gelai, depth of earthquakes decreases to

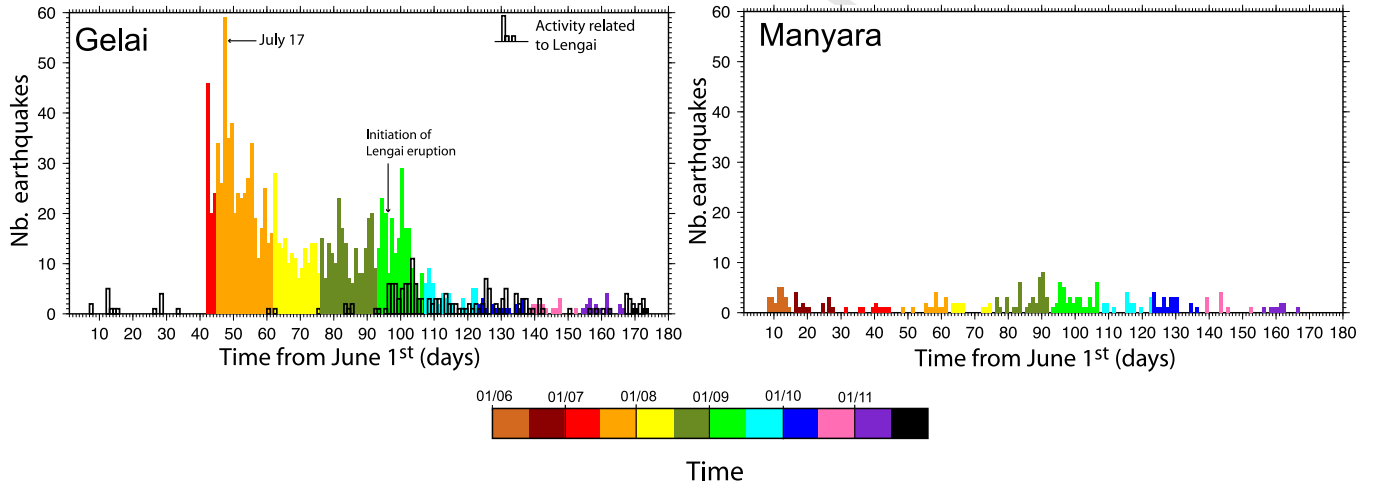



**Fig. 5.** Time histograms of the Gelai (left) and Manyara (right) earthquake sequences. On the Gelai time histogram, the black bars refer to the seismicity below the Oldoinyo Lengai volcano and the coloured ones to the Gelai sequence. Colour changes every half month, from 1st of June to November 30. The seismic activity under Gelai starts on September 12 and is maximum on July 17. The eruption of the Oldoinyo Lengai is marked by a renewal of activity under the volcano. The seismic rate is relatively stable at Manyara but probably underestimated from July to mid-August, because of the mask effect of the Gelai crisis.

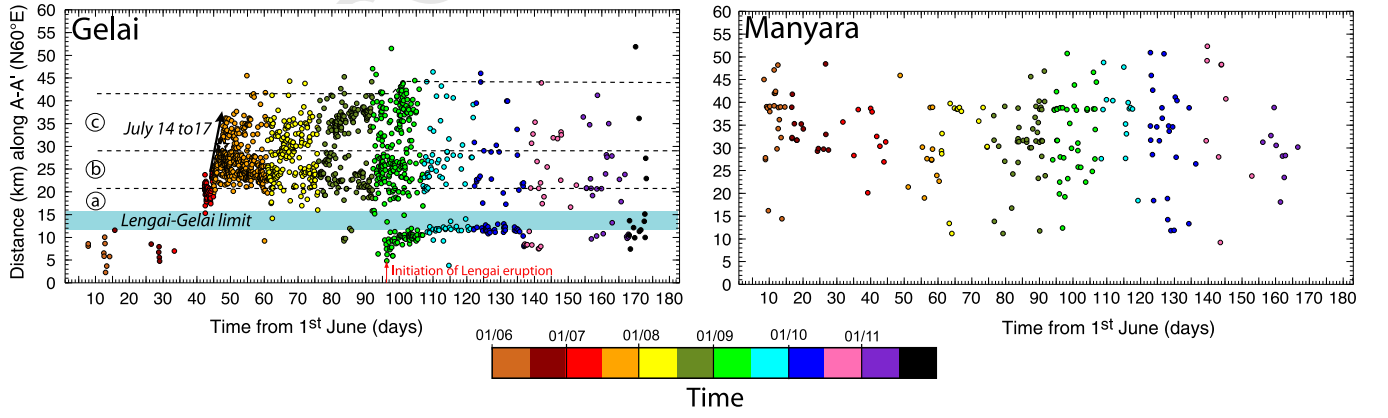



**Fig. 6.** Time distribution of the Gelai (left) and Manyara (right) earthquake sequences along N60°E direction (A–A' in Fig. 4). Colour changes every half month, from 1st of June to November 30. The distance between the Oldoinyo Lengai and the Gelai clusters is underlined by a blue band. The earthquakes below the Gelai volcano depict three areas annotated a, b and c (see text for details). The black arrow is related to the migration of the events from July 14 to 17 and the red one points out the initiation of the Oldoinyo Lengai eruption. The $M_w$ 5.9 earthquake is represented by a white star. (For interpretation of the references to colour in this figure legend, the reader is referred to the web version of this article.)

Please cite this article in press as: Albaric, J., et al. Contrasted seismogenic and rheological behaviours from shallow and deep earthquake sequences in the North Tanzanian Divergence, East Africa. J. Afr. Earth Sci. (2009), doi:10.1016/j.jafrearsci.2009.09.005

the N–E, from about 13 km to the surface (Fig. 4C). The maximum depth frequency is between 5 and 10 km (Fig. 4G).

The time distribution of the earthquakes in the N60°E direction reveals three major earthquake concentrations under the Gelai region (Fig. 6). From July 12 to 14, seismicity is limited to the southwestern end of the entire cluster (annotated (a) in Fig. 6) and propagates upward for ~10–15 km in the N–E direction between July 14 and 17, before the occurrence of the main event (black arrow and white star in Fig. 6). Then, two distinct areas of seismicity appear with the southern one more active till the beginning of August (annotated (b) and (c) in Fig. 6). The combined analysis of data from the seismicity recorded in July, global positioning system (GPS), radar interferometry and field observations, has shown that most of the strain recorded during the main crisis period was released aseismically (Calais et al., 2008). Indeed, slow slip occurred on a NW-dipping normal fault from July 12 to 17 which then led to the triggering of a magmatic intrusion by static stress change (Calais et al., 2008). From mid-August, the interferograms reveal surface deformation on the eastern and southern sides of the Gelai volcano (see Fig. 3(f) and (g) in Baer et al., 2008). The location of the seismicity could be correlated to the three southern fault structures but not to the modelled N–W dyke segment inferred by Baer et al. (2008) for the time period.

#### 4.1.2. Magnitude and focal mechanism

The focal mechanism of the main event that occurred on July 17 ($M_w$ 5.9) indicates normal faulting (Calais et al., 2008, Fig. 4A and E). It was preceded by two earthquakes of $M_w$ 5.3 and 5.4 two days before, then followed by one earthquake of $M_w$ 5.3 four hours later and by two of $M_w$ 5.2 on July 18 and 26. The majority of the local magnitudes inferred from the coda picking ranges between 3.5 and 4, out of the limit of validation of the Lee formula (Lee et al., 1972, see Section 3.2).

#### 4.1.3. Waveforms and spectrograms

We have recorded two different types of earthquakes during the Gelai crisis, as shown by the two characteristic spectrograms at station KRTU (Fig. 7A and B). With a predominant frequency content of 4–12 Hz, event A is comparable to a tectonic event, called volcano-tectonic by Chouet (1996) considering the magmato-tectonic nature of the seismic crisis (Calais et al., 2008). Event B presents more similarities with an hybrid event (Chouet, 1996; Power et al., 2002), with a maximum of energy released in the 1–6 Hz range and a coda frequency peacked around 2 Hz.

#### 4.1.4. Activity of the Oldoinyo Lengai volcano

From June 18, a renewal of effusive activity was observed at the nearby carbonatitic Oldoinyo Lengai (Vaughan et al., 2008). More intense lava flows in August–September were reported, preceding an explosive eruption on September 4 (Vaughan et al., 2008). Seismic activity under the volcano was recorded since the beginning of the experiment. The earthquakes are arranged into two vertically separate swarms, at around 5 and 13 km depth (Fig. 4C). The deepest swarm is likely correlated to the second deep magma chamber proposed by Baer et al. (2008). The explosive eruption of the volcano is well illustrated by a concomitant increase of the number of earthquakes (Fig. 5), migrating eastward (Figs. 5 and 6). At the same time, the seismic activity is still important under Gelai. The earthquakes under the two volcanoes depict two distinct clusters separated from ~5 km. However, there is a geometrical connection between their depth distribution: the deepest cluster below Lengai is indeed at the junction between a vertical axis below Lengai and the SW-dipping line drawn by the Gelai sequence (Fig. 4C).

### 4.2. The Manyara earthquake sequence

#### 4.2.1. Spatial and time distribution

The southern end of Lake Manyara is the second region where we have recorded a large amount of earthquakes. It coincides with the limit between two main normal faults, the segmented end of the ~N10° East-dipping Manyara fault and the ~N50° SE-dipping Balangida fault (Figs. 1 and 4B). With 0–8 earthquakes per day, the seismic rate is continuous during the period of recording (Fig. 5). It is indeed a long-lasting activity, already observed 12 years ago by Nyblade et al. (1996) with a 1 year seismic regional experiment in 1994–1995 (Fig. 2).

The sequence comprises 211 well-located epicenters forming two elongated clusters, striking roughly N60°E (Fig. 4B). Most of the events are clustered between 24 and 32 km depth and absent above 15 km, in the upper crust. The earthquakes are arranged more or less vertically, with the northern cluster deeper than the

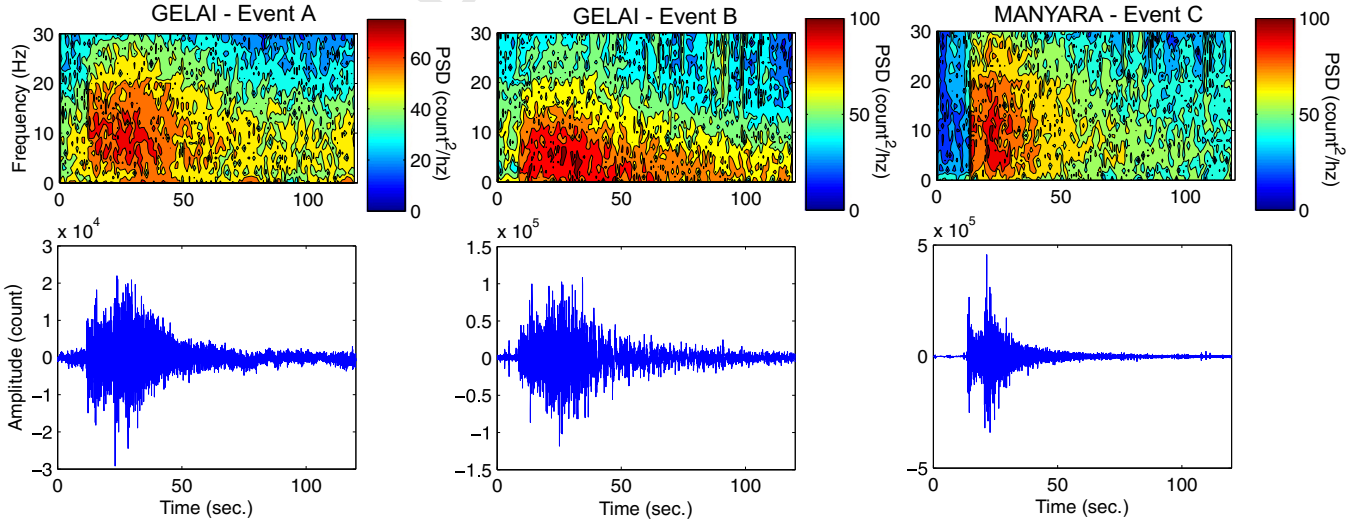



**Fig. 7.** Seismograms (vertical component) of 3 events in the Gelai (A and B at 87 km of epicentral distance and depth of 5.6 km) and Manyara (C at 47 km of epicentral distance and depth of 26.1 km) regions recorded at station KRTU. The spectrograms represent the Power Spectral Density (PSD) of each seismogram. The PSD scale is independent for each event. Events A and B ($M_L$ 3.6 and 4.1, respectively) are characterized by a long decay in time of the energy after the *S*-arrival which can be explained by the shallow depth. A shift in frequency from event A to B is observed with quite low frequencies in the coda for event B. Body waves and associated coda shape dominate event C record ($M_L$ 3.3).

Please cite this article in press as: Albaric, J., et al. Contrasted seismogenic and rheological behaviours from shallow and deep earthquake sequences in the North Tanzanian Divergence, East Africa. J. Afr. Earth Sci. (2009), doi:10.1016/j.jafrearsci.2009.09.005

other one (Fig. 4F). According to their time distribution, the hypocenters did not migrate in a particular direction (Figs. 4 and 6).

#### 4.2.2. Magnitude and b-value

No large historical earthquakes have been identified in the locus where the sequence has occurred. Local magnitudes, inferred from coda picking, vary from 1.6 to 3.6, but most of them range between 2.5 and 3. The *b*-value estimated with the Maximum Likelihood method is 1.48 (Aki, 1965). Considering the limited magnitude range used here, it is not well constrained enough to be accurately interpreted.

#### 4.2.3. Waveforms and spectrograms

All the earthquakes recorded show impulsive *P* and *S* phases and their high spectral content of 5–15 Hz is typical of a tectonic event (Fig. 7C).

### 4.3. Conclusion on the Gelai and Manyara sequences

From the above descriptions, the Gelai and Manyara sequences present major differences regarding:

- the depth frequency distribution of earthquakes: maximal at 5–10 km for Gelai and 24–32 km for Manyara;
- the variation of the seismicity rate: increase and decrease for Gelai and continuous for Manyara;
- the relative time-distribution of epicenters and hypocenters: migration NE for Gelai and stationary for Manyara;
- the presence of a large event: $M_w$ 5.9 at Gelai and none at Manyara;
- the occurrence of another type of natural phenomenon in the vicinity of the sequences: the eruption of the Oldoinyo Lengai volcano for Gelai and none for Manyara.

There is however one noticeable similitude between them: the long-axis of their elongate cluster around N60°E, comparable to the strike of the $M_w$ 5.9 event of July 17, 2007.

None of these two sequences presents the "swarm" or "main-shock–aftershock" patterns (Mogi, 1963), with an hybrid case at Gelai and a long-lasting-cluster type at Manyara. Separate processes are thus assumed to have triggered these sequences. In comparison with the aseismic deformation at Gelai, the Manyara sequence looks like background seismicity related to a long-term process.

## 5. Inferences on the crustal rheology

### 5.1. Depth distribution of earthquakes recorded

Depth frequency distribution of earthquakes has often been used to investigate thermo-mechanical properties of the crust (Meissner and Strehlau, 1982; Maggi et al., 2000; Déverchère et al., 2001). Indeed, earthquakes are not equally distributed in the crust: their proportion increases and decreases around one main peak of seismicity. In the case of well-located and large enough data sets, the latter can be correlated to the upper limit of the brittle-to-ductile transition (BDT) (Albaric et al., 2009, and references therein).

In the EARS, Albaric et al. (2009) have examined the depth frequency distribution of earthquakes from various catalogues of seismicity, and have shown relative variations along the Eastern Branch of the rift with a peak of seismicity deeper from N to S. However, their results were limited by the small amount of data in the NTD and their relative inaccuracy.

From our new data set we observe the same tendency: depth distribution of the Gelai and Manyara sequences are completely different, with a maximum of seismicity in the upper and lower parts of the crust, respectively. Gelai region is just at the limit between the narrow Kenya rift and the NTD, and the distribution of earthquakes in the crust is comparable to the swarm observed by Ibs-von Seht et al. (2001) just a few hundred kilometers north, below Lake Magadi (Fig. 2), and to the seismicity recorded at Lake Bogoria in 1985 (Young et al., 1991), with most of hypocenters above 10–15 km (Fig. 4G).

Hypocenters are above 15 km depth under the volcanic transverse belt and below 20 km, for most of them, south of 3.3°S between the lakes Eyasi and Manyara (Mbulu domain) (Fig. 1A and Fig. 8). Deep crustal earthquakes have already been evidenced (Shudofsky et al., 1987; Seno and Saito, 1994; Foster and Jackson, 1998; Brazier et al., 2005), but more as isolated cases while it concerns here the majority of the events.

### 5.2. Computation of a yield stress envelope

Comparing depth frequency distribution of earthquakes with stress changes in the crust supposes that distribution is representative to the long-term strength of the crust (Déverchère et al., 2001). In order to model a yield stress envelope (YSE (MPa)), the

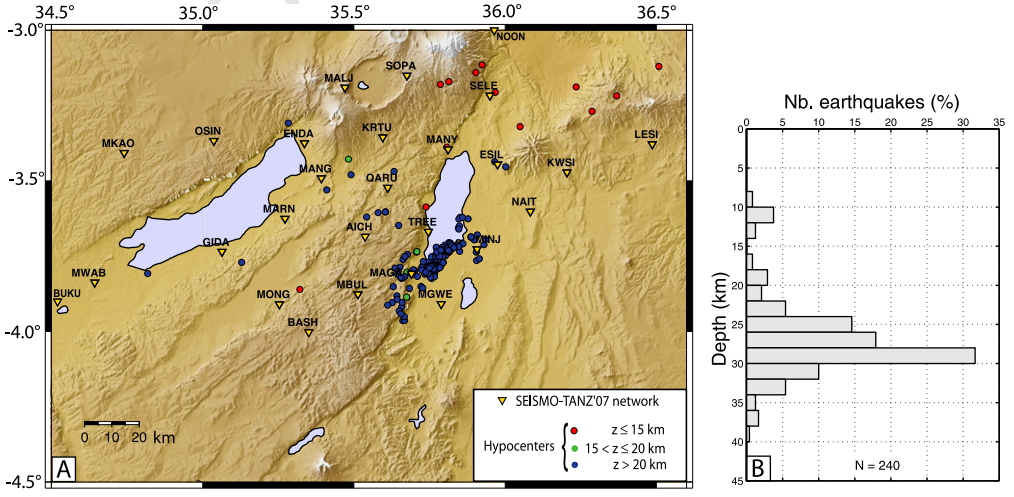



**Fig. 8.** (A) Map of the North Tanzanian Divergence (NTD) with earthquakes used in the YSE modelling. A colour code is associated to the depth range of the hypocenters. Depth of earthquakes increases from N to S: events are above 15 km under the transverse volcanic belt and deeper than 20 km south of 3.3°S. (B) Depth distribution of earthquakes plotted in A. The data set includes events located with the traditional absolute location approach (selected with depth error ⩽2 km and gap ⩽180°) and the 211 relocated earthquakes of the Manyara sequence (Fig. 4B). *N*, number of earthquakes.

Please cite this article in press as: Albaric, J., et al. Contrasted seismogenic and rheological behaviours from shallow and deep earthquake sequences in the North Tanzanian Divergence, East Africa. J. Afr. Earth Sci. (2009), doi:10.1016/j.jafrearsci.2009.09.005

UNCORRECTED PROOF

procedure applied here consists in adjusting crustal physical composition parameters to fit strength percentage (YSE (%)) with known focal distribution of earthquakes (Déverchère et al., 2001; Albaric et al., 2009). The YSE is computed with empirical deformation laws describing the brittle (Eq. (1)) and ductile (Eq. (2)) behaviour of the lithosphere (Sibson, 1974; Ranalli, 1995):

$$(\sigma_1 - \sigma_3)(z) = \alpha \rho g z (1 - \lambda) \quad (1)$$

$$(\sigma_1 - \sigma_3)(z) = \left(\frac{\dot{\epsilon}}{A^*}\right)^{1/n} \cdot e^{\frac{E}{nRT(z)}} \quad (2)$$

$\sigma_1$ and $\sigma_3$ are the maximum and minimum normal principal stress (MPa), respectively. $\alpha$ is a factor depending on fault type equal to 0.5 in the case of normal faulting (Ranalli, 1995). $\lambda$ is the ratio of pore fluid pressure to overburden pressure (0.4 for the EARS, Fadaie and Ranalli, 1990 and references therein), $g$ the acceleration due to gravity and $z$ the depth (km). $\dot{\epsilon}$ is the steady state-strain rate ($10^{-15}$ $s^{-1}$ from, Ebinger, 1989), $T(z)$ the temperature (K) and $R$ the gas constant. A steady-state geotherm $T(z)$ is computed (Turcotte and Schubert, 2002) for a surface heat flow of 46 mW $m^{-2}$ (Nyblade, 1997) and $T(0) = 0$°C. Density $\rho$(kg $m^{-3}$), constant $A^*$ (MPa$^{-n}$ $s^{-1}$), activation energy $E$(kJ $mol^{-1}$) and power law exponent $n$, are material parameters from Ranalli (1997), Turcotte and Schubert (2002) and Afonso and Ranalli (2004).

By varying the composition and thickness of crustal layers we obtain the YSE (MPa) and calculate the strength percentage YSE (%) each 2 km and compare it with the earthquakes distribution at same depth. We took the average value of 40 km for the crustal thickness (Last et al., 1997) in order to compare our results with modelling made by Albaric et al. (2009).

The earthquakes selected for the modelling comprise the relocated Manyara sequence and events located in the NTD with gap $\leqslant 180°$ and error on depth $\leqslant \pm 2$ km (Fig. 8). Because the Manyara sequence seems to be related to a long-term phenomenon and does not include large events, no declustering was involved.

Best fit between YSE (%) and percentage of earthquakes, given the panel of composition used, is obtained for a crust composed of 20 km of granite in its upper part, and of 20 km of wet-diabase in its lower part (Fig. 9A). The envelope (YSE (MPa)) is comparable with the one inferred by Albaric et al. (2009) in the same region (Fig. 9B).

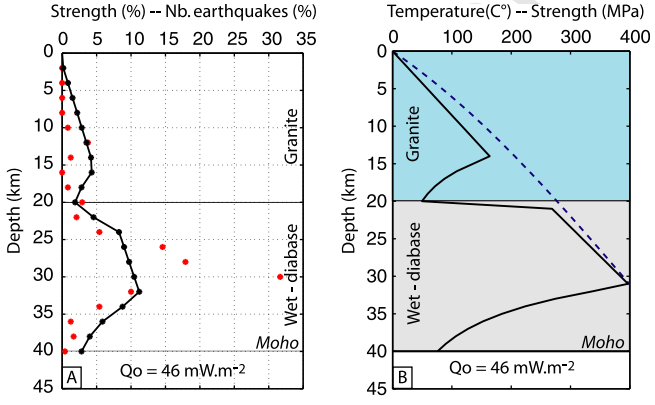



**Fig. 9.** Modelling of a yield stress envelope (YSE) representative of the NTD region. (A) Comparison between the calculated strength percentage (black points joined up by line) and the percentage of seismicity (red points, see Fig. 8 for the event selection) per 2 km depth interval. For example, at 22 km depth, the red point refers to the percentage of events that occur in the layer 20–22 km and the black one to the contribution of this layer in the total strength of the crust. The approach consists in fitting the strength percentage as well as possible to the seismicity percentage by testing different compositions of the crust: the best fit is obtained for a crust composed of 20 km of granite and 20 km of wet-diabase. (B) Yield stress envelop (MPa) deduced from modelling with the seisimicity-strength comparison approach described in (A). $Q_o$ is the surface heat flow used to compute the steady-state geotherm (blue dashed line on B). (For interpretation of the references to colour in this figure legend, the reader is referred to the web version of this article.)

## 6. Discussion

During the period of the SEISMO-TANZ' 07 seismological experiment, we have recorded a diffuse seismicity in the North Tanzanian Divergence (NTD) and two major earthquake sequences, called here Gelai and Manyara, located at the northern limit and in the NTD, respectively (Fig. 1A). Although occurring in two distinct rift settings, these sequences display common geometrical features and also contrasted patterns that open issues regarding structures and geodynamics of the EARS, for instance strain/magmatism relationships, structural inheritance, and rheological control on deformation. We highlight and discuss here the main preliminary consequences of these patterns of seismicity with respect to the EARS structure and dynamics and to some other seismicity sequences in the world.

### 6.1. Structural implications

The two seismic sequences clearly draw in map view a ca. 10 × 20 km elliptic-shaped zone, with a long axis oriented approximately NE–SW. Therefore the corresponding magmatic and/or fault active structures appear to trend obliquely to the general N–S trend of the rift axis (Fig. 1). This direction is also found in the strike of the largest earthquake recorded during the Gelai crisis, where the combined analysis of three types of geophysical data has highlighted a fault plane striking NE–SW, dipping 60° to the N–W, at depths from 2 to 14 km (Calais et al., 2008). No direct fault-induced scarps are associated to the faulting event at the surface. At a larger scale, the structural sketch map of Fig. 1 suggests that the Gelai sequence lies at the NE end of a major NE–SW transverse rift structure, the so-called Eyasi-Gelai lineament, running over 400 km from the Eyasi master fault tip zone to the Ngorongoro-Gelai volcanic alignment. The Manyara seismic sequence also outlines a NE–SW strike close to the southern shoreline of Lake Manyara, still without any significant topographic expression. The detailed map distribution of the Manyara seismicity shows two parallel narrow strips of earthquakes, striking N60°E, with a spacing of a few kilometeres, and displaying respective lengths of 20 km (northern one) and 10 km (southern one) (Fig. 10A). On the cross-section perpendicular to this direction they form two discrete vertical structures cutting the crust in the depth range 22–30 km (south) and 27–38 km (north) (Fig. 10B).

With respect to the Manyara–Balangida extensional linked fault system, the Manyara earthquakes occur in the immediate hanging-wall domain, north of the relay zone between the highly segmented N10°-striking Manyara fault structure to the N, and the more linear N50°-oriented Balangida fault structure to the S (Fig. 10A). Because of such a specific location, two alternative structural models can be proposed about the origin of the Manyara earthquakes with respect to rift versus basement fabrics.

The first hypothesis implies that the Manyara exposed fault scarp should connect at depth to the hypocenter zone with two possible fault trajectories (Fig. 10C). (1) The downward-projected extent of the Manyara fault into the discrete vertical seismic structures results in an unlikely fault profile, steepening at depth from ca. 65° to 80° (Fig. 10C, planar fault profile). (2) Assuming that the clusters are part of a thick infracrustal extensional detachment along which the Manyara master fault could root at depth implies low-angle seismically active shear zones with displacement top-to-the-east (Fig. 10C, listric fault profile). The latter are not consistent with the steep attitude of the clusters (Fig. 10A). In both cases,

CORRECTED PROOF

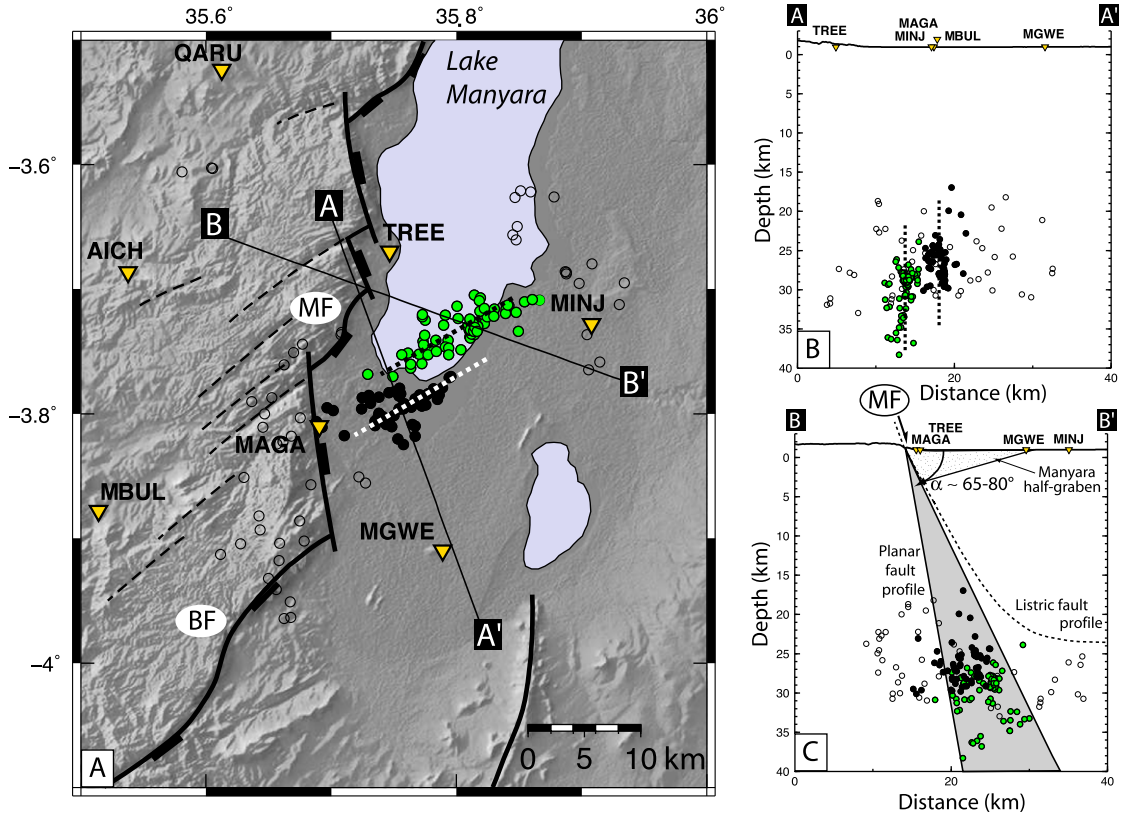



**Fig. 10.** (A) Map of the seismicity in Lake Manyara. Thick lines delineate major faults and thin dashed ones the main N–E direction. Green and black circles refer to two distinguishable clusters while the rest of the seismicity is plotted with empty circles. The earthquakes are aligned along the N60°E direction (dashed line across clusters). (B) Cross-section perpendicular to the direction of the clusters (A–A′ on A). Earthquakes are arranged along two vertical zones (dashed lines) between ~25 and 40 km for the northern one (green circles) and between ~20 and 30 km for the southern one (black circles). (C) Cross-section perpendicular to the mean direction of the segmented Manyara fault (B–B′ on A). The latter is projected downward into the earthquake sequence either as planar (thick line) or as listric (dashed line) profile. The "planar fault" hypothesis implies a fault surface dip in the range 65–80°, according to the location of the earthquakes. MF, Manyara fault; BF, Balangida fault.

the lack of earthquakes through the 20 km of crustal section cut by the uppermost part of the inferred fault plane is not a typical character of seismogenic fault structures.

Lastly, in map view, the high angle of obliquity (30–40°) between the surface trace of the fault and the projected seismic lineaments should imply that two en echelon fault segments formed at depth along a ca. NS-trending dextral shear zone joining the Manyara fault at the surface. However, this hypothesis is not supported by kinematic and geophysical data about the Manyara bounding fault structure that both suggest a dominant dip-slip motion (Ebinger et al., 1997; Le Gall et al., 2008). According to the second hypothesis, the Manyara earthquake sequence should occur along steeply-dipping rejuvenated basement structures that extend in the NE prolongation of NE–SW-oriented linealry structures, either cutting through the Balangida basement footwall block, or forming fault segments of the Balangida bounding fault (Fig. 10). A number of these pre-rift structures might have formed as Late Proterozoic shear zones post-dating ductile fabrics in the Mozambique frontal belt during the late collisional stage at 630–440 Ma, similarly to parallel dextral shear zones documented further south in the Proterozoic basement of the Lake Malawi rift (Ring, 1994). The overall pattern of NE–SW dextral shear zones is likely to have developed as conjugate structures, synchronously to the prominent NW–SE left-lateral shear zones of ASWA-type, known to have locally guided the geometry of rifting in Kenya (Berhe, 1990; Smith and Mosley, 1993; Coussement, 1995). A similar pattern of earthquake sequence located at the crosscut of inherited structures guiding the rift opening is found in the north Baikal rift (Déverchère et al., 1993). The absence of seismicity along the Balangida fault would imply that only the deepest part of the Late Proterozoic shear zones have been seismically reactivated.

### 6.2. Triggering mechanisms of sequences and comparison to other sequences

The two earthquake sequences, Gelai and Manyara, captured in 2007 are only at ~150 km distance and do not depict obvious genetic links (Fig. 4). Except their elongated shape in the same direction, they are mostly characterized by contrasted differences (in depth, time and space distributions, frequency content, magnitudes, see Figs. 4–7). We therefore anticipate that they may have distinct origins that we attempt here to clarify by comparing briefly these sequences to other ones.

The pattern observed at Gelai indicates neither a swarm-like nor a mainshock–aftershock sequence, as also reported in many other seismo-magmatic settings (e.g., Sherburn, 1992; Ukawa and Tsukahara, 1996; Toda et al., 2002; Hurst et al., 2008). It is rather a continuum between swarms and mainshocks, with highly variable time patterns. The Gelai crisis was identified as a sequence of events including slow slip on normal fault and dyking, instruments of the strain accommodation in continental rifting (Calais et al., 2008). In a comparable study in Afar, deformation observed in a rift segment has been explained by the injection of two lateral dykes, thanks to the analysis of seismic, geodetic and field data sets (Keir et al., 2009). The Afar and Gelai events are both dominated by aseismic processes. However, there was no slow slip in the case of the Afar. The dyke dimensions modelled in the two studies are comparable (about 10 km long and 2 m wide). Difference in the

Please cite this article in press as: Albaric, J., et al. Contrasted seismogenic and rheological behaviours from shallow and deep earthquake sequences in the North Tanzanian Divergence, East Africa. J. Afr. Earth Sci. (2009), doi:10.1016/j.jafrearsci.2009.09.005

deformation mechanism between the Afar and the Gelai events is reflected in their associated earthquake sequences. Their time duration is in the order of several months for Gelai and only days for swarms in Afar. A large event ($M_w$ 5.9) occurred at Gelai while the highest magnitude earthquake recorded in Afar was $M_L$ 4.7. In addition, normal faulting may have played a greater role in the Gelai crisis as suggested by the comparison between the seismicity and the fault structures modelled by Baer et al. (2008) from mid-August. These different mechanisms probably arise from the advanced and early stages of rifting, respectively, in Afar and northern Tanzania, and from the structural inheritance.

Note that this sequence was also followed by a volcanic eruption in a neighbouring edifice, the Oldoinyo Lengai (Figs. 4A, 5, 6), below which dense shallow and deep swarms are identified (Fig. 4C). Baer et al. (2008) pointed out a temporal and spatial correlation between the Gelai and Oldoinyo Lengai volcanoes. The authors proposed either a pressure drop after the dyking event or a dynamic triggering of the Oldoinyo Lengai eruption by the seismicity of Gelai, suggesting that the passage of seismic waves through the Oldoinyo Lengai magma chamber would have promoted the bubbles growth, and thus increased the magma buoyancy. A temporal link of the same order could have persisted later, with the occurrence of earthquakes of relatively high magnitude in December and the eruption of the Oldoinyo Lengai in February and March 2008 (Global Volcanism Program, 2009). While there is a gap of seismicity of ~5 km between the two volcanoes, they depict a spatial continuity owing to the clear alignment of the deepest swarm below Oldoinyo Lengai with the S–W trending Gelai sequence (Fig. 4C). Therefore, our results further strengthen a spatial and temporal association of the magmatic and tectonic events observed at Gelai and Lengai during the whole crisis.

The case of Manyara appears more enigmatic in the sense that it has been rarely observed for a sequence to last over more than 10 years, as suspected from Nyblade et al. (1996)'s study.

There is apparently no migration of the sequence through space or time, and no large historical event known. It is rather similar to the Busingol earthquake sequence, southernmost Baikal rift (Zhalkovskii et al., 1995; Delouis et al., 2002), revealing a process of long-lasting stress loading without main shock in a more than 10 years time window. Although the *b*-value found here (~1.5) is questionable because of the limited magnitude range (2.5–3), a high *b*-value (~1.3) is also found in the Busingol case (Ayunova et al., 2007). Note that the Busingol crisis ended by a $M_w$ 6.3 event in December 1991 (Bayasgalan et al., 2005). In contrast to the Gelai region, there is no eruption or strongly anomalous thermal events reported in the Manyara segment. A process of stress loading in pre-fractured zones of high strength in the crust induced by rift propagation and/or block rotation can be invoked to explain such a duration of the sequence.

However, the Manyara basin is located in the northern alignment of the recent Kwaraha volcanic province (Bagdasaryan et al., 1973) and may therefore depict thermally weakened portions of the crust, thus prone to focus strain. Such weakening effects are proposed in some swarms of the Baikal rift from a correlation with hydrothermal sources (Kuzmina, 2007). Lower crustal earthquakes in active rifts could also occur in a brittle regime with high pore pressure as proposed by Seno and Saito (1994). In continental rifts settings, deep fluids have been proposed to drive low-crustal seismicity around dry, mafic crust, as in the rifted crust of the Taupo Volcanic zone of New Zealand (Reyners et al., 2007). Such a mafic composition is also favoured by massive dyke injection, as involved in Lake Tahoe, California (Smith et al., 2004). Indeed, magmatic intrusions could lead to increase locally the strain rate at these great depths, which is required to trigger earthquakes, and to strengthen the crust (Smith et al., 2004). Both factors may play a role in the deep seismicity reported here, although the time distribution of events and the propagation pattern may be different among these active rift zones.

### 6.3. Rheological implications

Another important result is the influence of rheology on the depth level of seismicity peaks. The sensitivity of depth distribution of earthquakes to thermal gradients and composition of the crust is demonstrated since long, especially in the EARS (Shudofsky et al., 1987; Foster and Jackson, 1998; Albaric et al., 2009). From these studies, it appears that the presence of a mafic lower crust and the level of thermal disturbance by Cenozoic rifting both play a key role on the seismicity depth distribution. We lack accuracy on hypocenters in the Gelai sequence to discuss the depth distribution in terms of rheology. We note however that the depth range of events in Gelai (Fig. 4G) is similar to the one found in the 1985 Lake Bogoria sequence (Young et al., 1991). Both curves tend to depict a unique shallow peak of seismicity, revealing a "weak" strength profile characterized by a brittle-ductile transition (BDT) beginning at 10 km depth and a maximum strength of only 120 MPa, and no strength in the lower crust (Albaric et al., 2009). Earthquakes located in the NTD (coming mostly from the Manyara sequence) provide a more favourable database in this respect because the SEISMO-TANZ' 07 network is ideally disposed to constrain depths and because it represents a long-lasting sequence, supposed to "illuminate" the BDTs and zones of high strength more accurately. The events located in the Mbulu area depict a pattern that requires a strong, mafic lower crust, a granite-type weak upper crust, and a rather "cold" geotherm (Figs. 8, 9A and B). The poor fit in amplitude for the deepest peak (Fig. 9A) can be explained by the fact that the Manyara sequence over samples the lower crust seismicity compared to the upper crust one in this time window. These results confirm both the strength increase of the crust from Kenya to the south of the NTD and the mafic composition of the lower crust inferred by Albaric et al. (2009). In addition, this mafic composition is consistent with the high velocities of the deepest part of the lower crust observed in south Kenya by seismic refractions studies (Birt et al., 1997).

A westward deep upper mantle anomaly has been identified from Ethiopia to Tanzania (Ritsema et al., 1998; Benoit et al., 2006; Park and Nyblade, 2006). However, the contrast in the volcanic activity between the Gelai and the Manyara regions and the depth of the BDT suggest that some parts of the contact of the Tanzanian craton to the Proterozoic belts may be yet preserved from the thermal disturbance in the deep upper mantle.

## 7. Conclusion

The Gelai and Manyara earthquake sequences (eastern branch of the EARS, southern tip) emphasize the preferred locus of active strain release along NE–SW discontinuities which probably root at depth into steep Proterozoic shear zones. Zones of maximal strength are dependent both on this inherited fabrics and on the thermal disturbances induced by the Cenozoic rifting, explaining the contrasted depths of strain focusing. We therefore find that a strong structural control is exerted both at local and large scales by the basement on the overall rift propagation path throughout the NTD (Le Gall et al., 2004; Macheyeki et al., 2008). This discontinuous belt of active strain has been recently assimilated to the Victoria–Somalia micro-plate boundary (Calais et al., 2006; Stamps et al., 2008).

The NTD is characterized by a deep seismic activity, with about 10 years-lasting sequence in the region of Manyara. Cold geotherm computed with low surface heat flow observed in the region (Nyblade, 1997) and mafic lithologies are required to model a yield

UNCORRECTED PROOF

Please cite this article in press as: Albaric, J., et al. Contrasted seismogenic and rheological behaviours from shallow and deep earthquake sequences in the North Tanzanian Divergence, East Africa. J. Afr. Earth Sci. (2009), doi:10.1016/j.jafrearsci.2009.09.005

stress envelope from the depth frequency distribution of earthquakes observed in the Mbulu domain (Eyasi-Manyara). Our results also confirm the spectacular increase in the strength of the lower crust from south Kenya to NTD (Albaric et al., 2009).

The comparison between the two earthquake sequences underlines different deformation processes at ~150 km distance. The Gelai crisis is dominated by aseismic processes (Calais et al., 2008) but probably also influenced by classic normal faulting and structural inheritance. Spatial and temporal correlations are observed between the seismicity under the active Oldoinyo Lengai and the Gelai volcanoes. The Manyara sequence does not depict the typical pattern of a seismic crisis but seems related to a long-term process maybe controlled by stress loading transmitted laterally. Episodic magmatic intrusions, though not recorded, might occur and favour a high strength lower crust.

## Acknowledgments

We acknowledge founding by INSU-CNRS DyeTI and 'Action de Suivi' Programs and by SRI (Service des Relations Internationales) of UBO (Brest University). We thank E. Calais for useful comments during this project and R. Lataste (French Embassy) and E. Mbede (Dar-Es-Salaam University) for supporting our experiment. We also thank the TANAPA (Tanzania National Parks), Ngorongoro Conservation Area Authority (NCAA), and the Tanzanian Geological Survey authorities which have allowed us to perform this study. We thank D. Keir, M. Ibs-von Seht and C. Ebinger who helped improve this manuscript.

## References

Afonso, J.C., Ranalli, G., 2004. Crustal and mantle strengths in continental lithosphere: is the jelly sandwich model obsolete? Tectonophysics 394 (3–4), 221–232.

Aki, K., 1965. Maximum likelihood estimate of $b$ in the formula $\log N = a - bM$ and its confidence limits. Bulletin of Earthquake Research Institute 43, 237–239.

Albaric, J., Déverchère, J., Petit, C., Perrot, J., Le Gall, B., 2009. Crustal rheology and depth distribution of earthquakes: insights from the central and southern East African Rift System. Tectonophysics 468 (1–4), 28–41.

Ayunova, O.D., Kalush, Y.A., Loginov, V.M., 2007. Relationship of the seismic activity of the Tuvinian and adjacent Mongolian areas with the fractal dimensionality of a fault system. Russian Geology and Geophysics 48 (7), 593–597.

Baer, G., Hamiel, Y., Shamir, G., Nof, R., 2008. Evolution of a magma-driven earthquake swarm and triggering of the nearby Oldoinyo Lengai eruption, as resolved by InSAR, ground observations and elastic modeling, East African Rift, 2007. Earth and Planetary Science Letters 272 (1–2), 339–352.

Bagdasaryan, G.P., Gerasimovskiy, V.I., Polyakov, A.I., Gukasyan, R.K., Vernadskiy, V.I., 1973. Age of volcanic rocks in the rift zones of East Africa. Geochemistry International 10, 66–71.

Baker, B.H., Mitchell, J.G., 1976. Volcanic stratigraphy and geochronology of the Kedong–Olorgesailie area and the evolution of the South Kenya rift. Journal of the Geological Society 132 (5), 467–484.

Barth, H., 1990. Provisional geological map of the Lake Victoria goldfields, Tanzania (1:500 000). Geologisches Jahrbuch Reihe B, 72.

Bayasgalan, A., Jackson, J., McKenzie, D., 2005. Lithosphere rheology and active tectonics in Mongolia: relations between earthquake source parameters, gravity and GPS measurements. Geophysics Journal International 163, 1151–1179.

Benoit, J.P., McNutt, S.R., 1996. Global volcanic earthquake swarm database and preliminary analysis of volcanic earthquake swarm duration. Annali Di Geofisica XXXIX (2), 221–229.

Benoit, M.H., Nyblade, A.A., VanDecar, J.C., 2006. Upper mantle P-wave speed variations beneath Ethiopia and the origin of the Afar hotspot. Geology 34 (5), 329–332.

Berhe, S.M., 1990. Ophiolites in Northeast and East Africa: implications for Proterozoic crustal growth. Journal of the Geological Society of London 147, 41–57.

Birt, C., Maguire, P., Khan, M., Thybo, H., Keller, G., Patel, J., 1997. The influence of pre-existing structures on the evolution of the southern Kenya Rift Valley – evidence from seismic and gravity studies. Tectonophysics 278 (1–4), 211–242.

Brazier, R.A., Nyblade, A.A., Florentin, J., 2005. Focal mechanisms and the stress regime in NE and SW Tanzania, East Africa. Geophysical Research Letters 32, L14315.

Brazier, R.A., Nyblade, A.A., Langston, C.A., Owens, T.J., 2000. Pn wave velocities beneath the Tanzania craton and adjacent rifted mobile belts, East Africa. Geophysical Research Letters 27 (16), 2365–2368.

Calais, E., d'Oreye, N., Albaric, J., Deschamps, A., Delvaux, D., Déverchère, J., Ebinger, C., Ferdinand, R.W., Kervyn, F., Macheyeki, A.S., Oyen, A., Perrot, J., Saria, E., Smets, B., Stamps, D.S., Wauthier, C., 2008. Strain accommodation by slow slip and dyking in a youthful continental rift, East Africa. Nature 456, 783–787.

Calais, E., Ebinger, C., Hartnady, C., Nocquet, J.M., 2006. Kinematics of the East African Rift from GPS and earthquake slip vector data. Geological Society, London, Special Publications 259, 9–22.

Cerling, T.E., Powers, D.W., 1977. Paleorifting between the Gregory and Ethiopian rifts. Geology 5 (7), 441–444.

Chatelain, J., 1978. Etude fine de la sismicité en zone de collision continentale à l'aide d'un réseau de stations portables: la région Hindu–Kush–Pamir. Ph.D. thesis, Univ. Paul Sabatier, Toulouse.

Chouet, B.A., 1996. Long-period volcano seismicity: its source and use in eruption forecasting. Nature 380, 309–316.

Coussement, C., 1995. Structures transverses et extension continentale. Le rôle des zones de failles d'Assoua et TRM dans la cinématique néogène du système de rift est-africain. Ph.D. thesis, University of Brest, France.

Crossley, R., 1979. The Cenozoic stratigraphy and structure of the western part of the Rift Valley in southern Kenya. Journal of the Geological Society 136 (4), 393–405.

Crossley, R., Knight, R.M., 1981. Volcanism in the western part of the rift valley in Southern Kenya. Bulletin of Volcanology 44 (2), 117–128.

Dawson, J.B., 1992. Neogene tectonics and volcanicity in the North Tanzania sector of the Gregory Rift Valley: contrasts with the Kenya sector. Tectonophysics 204 (1–2), 81–83.

Delouis, B., Déverchère, J., Melnikova, V., Radziminovitch, N., Loncke, L., Larroque, C., Ritz, J.F., San'kov, V., 2002. A reappraisal of the 1950 (Mw 6.9) Mondy earthquake, Siberia, and its relationship to the strain pattern at the southwestern end of the Baikal rift zone. Terra Nova 14 (6), 491–500.

Déverchère, J., Houdry, F., Solonenko, N.V., Solonenko, A.V., Sankov, V.A., 1993. Seismicity, active faults and stress field of the North Muya region, Baikal Rift: new insights on the rheology of extended continental lithosphere. Journal of Geophysical Research 98 (B11), 19895–19912.

Déverchère, J., Petit, C., Gileva, N., Radziminovitch, N., Melnikova, V., San'kov, V., 2001. Depth distribution of earthquakes in the Baikal rift system and its implications for the rheology of the lithosphere. Geophysical Journal International 146 (3), 714–730.

Ebinger, C., Djomani, Y.P., Mbede, E., Foster, A., Dawson, J.B., 1997. Rifting Archaean lithosphere: the Eyasi–Manyara–Natron rifts, East Africa. Journal of the Geological Society 154 (6), 947–960.

Ebinger, C.J., 1989. Tectonic development of the western branch of the East African rift system. Geological Society of America Bulletin 101 (7), 885–903.

Engdahl, E.R., van der Hilst, R., Buland, R., 1998. Global teleseismic earthquake relocation with improved travel times and procedures for depth determination. Bulletin of the Seismological Society of America 88 (3), 722–743.

Evans, A., Fairhead, J., Mitchell, J., 1971. Potassium–Argon ages from the volcanic province of Northern Tanzania. Nat. Phys. Sci. 2229, 19–20.

Fadaie, K., Ranalli, G., 1990. Rheology of the lithosphere in the East African Rift System. Geophysical Journal International 102 (2), 445–453.

Foster, A.N., Jackson, J.A., 1998. Source parameters of large African earthquakes: implications for crustal rheology and regional kinematics. Geophysical Journal International 134 (2), 422–448.

Global Volcanism Program, 2009. Department of Mineral Sciences, National Museum of Natural History, Smithsonian Institute. URL <http://www.volcano.si.edu>.

Havskov, J., Ottemöller, L., 2008. SEISAN: the earthquake analysis software. For WINDOWS, SOLARIS, LINUX and MACOSX. Version 8.2. Department of Earth Science, University of Bergen, Norway.

Hollnack, D., Stangl, R., 1998. The seismicity related to the southern part of the Kenya Rift. Journal of African Earth Sciences 26 (3), 477–495.

Hurst, T., Bannister, S., Robinson, R., Scott, B., 2008. Characteristics of three recent earthquake sequences in the Taupo Volcanic Zone, New Zealand. Tectonophysics 452 (1–4), 17–28.

Ibs-von Seht, M., Blumenstein, S., Wagner, R., Hollnack, D., Wohlenberg, J., 2001. Seismicity, seismotectonics and crustal structure of the southern Kenya Rift – new data from the Lake Magadi area. Geophysical Journal International 146 (2), 439–453.

Ibs-von Seht, M., Plenefisch, T., Klinge, K., 2008. Earthquake swarms in continental rifts – a comparison of selected cases in America, Africa and Europe. Tectonophysics 452 (1–4), 66–77.

Julia, J., Ammon, C.J., Nyblade, A.A., 2005. Evidence for mafic lower crust in Tanzania, East Africa, from joint inversion of receiver functions and Rayleigh wave dispersion velocities. Geophysical Journal International 162 (2), 555–569.

Keir, D., Hamling, I.J., Ayele, A., Calais, E., Ebinger, C., Wright, T.J., Jacques, E., Mohamed, K., Hammond, J.O.S., Belachew, M., Baker, E., Rowland, J.V., Lewi, E., Bennati, L., 2009. Evidence for focused magmatic accretion at segment centers from lateral dike injections captured beneath the Red Sea rift in Afar. Geology 37 (1), 59–62.

KRISP Working Party, 1991. Large-scale variation in lithospheric structure along and across the Kenya rift. Nature 354, 223–227.

Kuzmina, E., 2007. To the estimation of paragenetic correlation between earthquake swarms and geothermal sources. In: Proceedings of the XXII All Russian Conference of Young Scientists "Lithosphere structure and geodynamics", April 24–29, 2007, Institute of the Earth's Crust of SB RAS, Irkutsk, pp. 39–40.

UNCORRECTED PROOF

Please cite this article in press as: Albaric, J., et al. Contrasted seismogenic and rheological behaviours from shallow and deep earthquake sequences in the North Tanzanian Divergence, East Africa. J. Afr. Earth Sci. (2009), doi:10.1016/j.jafrearsci.2009.09.005

Langston, C.A., Brazier, R., Nyblade, A.A., Owens, T.J., 1998. Local magnitude scale and seismicity rate for Tanzania, East Africa. Bulletin of the Seismological Society of America 88 (3), 712–721.

Last, R.J., Nyblade, A.A., Langston, C.A., Owens, T.J., 1997. Crustal structure of the East African Plateau from receiver functions and Rayleigh wave phase velocities. Journal of Geophysical Research 102 (B11), 24469–24484.

Le Gall, B., Gernigon, L., Rolet, J., Ebinger, C., Gloaguen, R., Nilsen, O., Dypvik, H., Deffontaines, B., Mruma, A., 2004. Neogene–Holocene rift propagation in central Tanzania: morphostructural and aeromagnetic evidence from the Kilombero area. Bulletin of the Geological Society of America 116 (3–4), 490–510.

Le Gall, B., Nonnotte, P., Rolet, J., Benoit, M., Guillou, H., Mousseau-Nonnotte, M., Albaric, J., Déverchère, J., 2008. Rift propagation at craton margin: distribution of faulting and volcanism in the North Tanzanian Divergence (East Africa) during Neogene times. Tectonophysics 448 (1–4), 1–19.

Lee, W., Bennet, R., Meagher, K., 1972. A method of estimating magnitude of local earthquakes from signal duration. U.S. Geological Survey.

Lienert, B., Havskov, J., 1995. A computer program for locating earthquakes both locally and globally. Seismological Research Letters 66, 26–36.

Macheyeki, A.S., Delvaux, D., Batist, M.D., Mruma, A., 2008. Fault kinematics and tectonic stress in the seismically active Manyara–Dodoma Rift segment in Central Tanzania – implications for the East African Rift. Journal of African Earth Sciences 51 (4), 163–188.

Maggi, A., Jackson, J.A., McKenzie, D., Priestley, K., 2000. Earthquake focal depths, effective elastic thickness, and the strength of the continental lithosphere. Geology 28 (6), 495–498.

Meissner, R., Strehlau, J., 1982. Limits of stresses in continental crusts and their relation to the depth-frequency distribution of shallow earthquakes. Tectonics 1 (1), 73–89.

Mogi, K., 1963. Some discussions on aftershocks, foreshocks and earthquakes swarms – the fracture of a semi-infinite body caused by an inner stress origin and its relation to the earthquake phenomena. Bulletin of Earthquake Research Institute 41, 615–658.

Nonnotte, P., Guillou, H., Le Gall, B., Benoit, M., Cotten, J., Scaillet, S., 2008. New K–Ar age determinations of Kilimanjaro volcano in the North Tanzanian diverging rift, East Africa. Journal of Volcanology and Geothermal Research 173 (1–2), 99–112.

Nyblade, A.A., 1997. Heat flow across the East African Plateau. Geophysical Research Letters 24 (16), 2083–2086.

Nyblade, A.A., Birt, C., Langston, C.A., Owens, T.J., Last, R.J., 1996. Seismic experiment reveals rifting of craton in Tanzania. EOS 77 (51), 517–521.

Nyblade, A.A., Brazier, R.A., 2002. Precambrian lithospheric controls on the development of the East African rift system. Geology 30 (8), 755–758.

Park, Y., Nyblade, A.A., 2006. P-wave tomography reveals a westward dipping low velocity zone beneath the Kenya Rift. Geophysical Research Letters 33 (7), 7311.

Parsons, T., 2008. Persistent earthquake clusters and gaps from slip on irregular faults. Nature Geoscience 1, 59–63.

Power, J., Jolly, A., Nye, C., Harbin, M., 2002. A conceptual model of the Mount Spurr magmatic system from seismic and geochemical observations of the 1992 Crater Peak eruption sequence. Bulletin of Volcanology 64 (3), 206–218.

Prodehl, C., Fuchs, K., Mechie, J., 1997. Seismic-refraction studies of the Afro-Arabian rift system – a brief review. Tectonophysics 278 (1–4), 1–13.

Prodehl, C., Jacob, A., Thybo, H., Dindi, E., Stangl, R., 1994. Crustal structure on the northeastern flank of the Kenya rift. Tectonophysics 236 (1–4), 271–290.

Ranalli, G., 1995. Rheology of the Earth, second ed. Chapman & Hall, London. pp. 413.

Ranalli, G., 1997. Rheology and deep tectonics. Annali Di Geofisica XL (3), 671–680.

Reyners, M., Eberhart-Phillips, D., Stuart, G., 2007. The role of fluids in lower-crustal earthquakes near continental rifts. Nature 446, 1075–1078.

Ring, U., 1994. The influence of preexisting structure on the evolution of the Cenozoic Malawi rift (East African Rift System). Tectonics 13, 313–326.

Ritsema, J., Nyblade, A.A., Owens, T.J., Langston, C.A., VanDecar, J.C., 1998. Upper mantle seismic velocity structure beneath Tanzania, east Africa: implications for the stability of cratonic lithosphere. Journal of Geophysical Research 103 (B9), 21201–21213.

Seno, T., Saito, A., 1994. Recent east african earthquakes in the lower crust. Earth and Planetary Science Letters 121, 125–136.

Shackleton, R.M., 1993. Tectonics of the lower crust: a view from the Usambara Mountains, NE Tanzania. Journal of Structural Geology 15, 663–671.

Sherburn, S., 1992. Characteristics of earthquake sequences in the Central Volcanic Region, New Zealand. New Zealand Journal of Geology and Geophysics 35, 57–68.

Shudofsky, G.N., Cloething, S., Stein, S., Wortel, R., 1987. Unusually deep earthquakes in East-Africa – constraints on the thermomechanical structure of a continental rift system. Geophysical Research Letters 14 (7), 741–744.

Sibson, R.H., 1974. Frictional constraints on thrust, wrench and normal faults. Nature 249, 542–544.

Smith, K.D., von Seggern, D., Blewitt, G., Preston, L., Anderson, J.G., Wernicke, B.P., Davis, J.L., 2004. Evidence for deep magma injection beneath Lake Tahoe, Nevada–California. Science 305, 1277–1280.

Smith, M., Mosley, P., 1993. Crustal heterogeneity and basement influence on the development of the Kenya Rift, East Africa. Tectonics 12 (2), 591–606.

Solonenko, A., Solonenki, N., Melnikova, V., Shteiman, E., 1997. The seismicity and earthquake focal mechanisms of the Baikal rift zone. Bull. Centres Rech. Elf Explor. Prod. 21, 207–232.

Stamps, D.S., Calais, E., Saria, E., Hartnady, C., Nocquet, J.M., Ebinger, C.J., Fernandes, R.M., 2008. A kinematic model for the East African Rift. Geophysical Research Letters 35, L05304.

Toda, S., Stein, R.S., Sagiya, T., 2002. Evidence from the AD 2000 Izu islands earthquake swarm that stressing rate governs seismicity. Nature 419, 58–61.

Turcotte, D.L., Schubert, G., 2002. Geodynamics, second ed. Cambridge University Press. p. 456.

Ukawa, M., Tsukahara, H., 1996. Earthquake swarms and dike intrusions off the east coast of Izu Peninsula, central Japan. Tectonophysics 253 (3–4), 285–303.

Vaughan, R.G., Kervyn, M., Realmuto, V., Abrams, M., Hook, S.J., 2008. Satellite measurements of recent volcanic activity at Oldoinyo Lengai, Tanzania. Journal of Volcanology and Geothermal Research 173 (3–4), 196–206.

Vidale, J.E., Shearer, P.M., 2006. A survey of 71 earthquake bursts across southern California: exploring the role of pore fluid pressure fluctuations and aseismic slip as drivers. Journal of Geophysical Research 111, B05312.

Waldhauser, F., 2001. hypoDD – a program to compute double-difference hypocenter locations. Tech. Rep., U.S. Geologic Survey Open-File Report.

Waldhauser, F., Ellsworth, W.L., 2000. A double-difference earthquake location algorithm: method and application to the northern Hayward fault, California. Bulletin of the Seismological Society of America 90 (6), 1353–1368.

Young, P.A.V., Maguire, P.K.H., Laffoley, N.D., Evans, J.R., 1991. Implications of the distribution of seismicity near Lake Bogoria in the Kenya rift. Geophysical Journal International 105 (3), 665–674.

Zhalkovskii, N.D., Kuchai, O.A., Muchnaya, V.I., 1995. Seismicity and some characteristics of the stress state of the earth's crust in the Altai–Sayan region. Geologiya i Geofizika (Russian Geology and Geophysics) 36 (10), 20–30. 16–25.

UNCORRECTED PROOF

Please cite this article in press as: Albaric, J., et al. Contrasted seismogenic and rheological behaviours from shallow and deep earthquake sequences in the North Tanzanian Divergence, East Africa. J. Afr. Earth Sci. (2009), doi:10.1016/j.jafrearsci.2009.09.005